

Relativistic few-body problem. II. Three-body equations and three-body forces

Franz Gross*

Department of Physics, Carnegie-Mellon University, Pittsburgh, Pennsylvania 15213

(Received 16 June 1982)

Examination of the sum of all ladder and crossed ladder exchanges between three particles leads to a set of relativistic three-body equations of the Faddeev type in which two of the three particles are restricted to their mass shell. The choice of which two particles are on shell at a given instant is uniquely determined by the requirement that they be spectators either before or after the interaction. It is shown that these equations satisfy the cluster property, and the two-body amplitudes which drive the equations are known in principle. Three-body unitarity is proved. Three-body forces which arise from the underlying dynamics are discussed, classified, and estimated numerically for a spinless example. It is found that the three-body forces tend to cancel to some extent, are sensitive to the details of the dynamics, and that contributions to such forces, primarily of relativistic origin, can be important.

[NUCLEAR STRUCTURE Relativistic Faddeev equations from ladder
and crossed ladder exchanges. Unitarity, cluster property, and three-
body forces.]

I. INTRODUCTION AND DIAGRAMMATIC DERIVATION OF THE EQUATIONS

In this paper we present relativistic Faddeev equations for three spinless particles.¹ It is assumed that the dynamics which should describe such a system is the sum of all ladder and crossed ladder diagrams describing meson exchange, and analysis of this class of diagrams leads to the idea that two of the three particles should be restricted to their mass shell. This eliminates the dependence of the amplitudes on the relative energies in a covariant way, and gives equations which depend only on two relative three-momenta as in the nonrelativistic case. The relativistic two body amplitudes which drive the equations always have one of the two interacting particles on shell, and a two body theory for these amplitudes has been given in Ref. 2, to be called I. The entire approach taken in this paper is a natural extension of the ideas discussed in I.

Working from the underlying dynamics, it is possible to treat three body forces in a consistent way, and considerable attention is devoted in this paper to a discussion of how this might be done. Three body driving terms are introduced from the beginning, and the composition and size of such terms is

discussed in Secs. III and IV. It is found that the three body forces are very sensitive to precisely how the dynamics is handled, and while naive examination of the diagrams suggests that they should cancel in leading order, we find that the cancellations are incomplete and that depending precisely on how the equations are treated, three body forces of purely relativistic origin could be important. This result is potentially very interesting, and unexpected. More work on this aspect of the problem is needed, and the realistic situation of spin $\frac{1}{2}$ particles needs to be investigated.

Our equations bear some resemblance to those introduced by Alessandrini and Omnes,³ who also considered a Green's function in which two particles were restricted to their mass shell, but in other respects their Green's function is different from ours. Their equation does not satisfy the cluster property; the two body amplitudes which drive their equation depend explicitly on the energy of the third particle in a nontrivial way. It is shown in Sec. II that our equation does satisfy the cluster property. We also show in Sec. II that elastic unitarity is satisfied, in common with other three body equations.¹ It appears that it would be straightforward to include bound states in the two body sectors, but this is not discussed in this paper, and will

be published elsewhere.

The remainder of this section is devoted to a diagrammatic derivation of the equations. An explicit algebraic form for the equations is given in Sec. II, where the proofs of three body unitarity and the cluster property are given. Section III enumerates the contributions to the three body irreducible kernel in lowest (sixth) order and presents some crude estimates of the size of the various terms at threshold. In Sec. IV the treatment of identical particles is discussed. Spurious singularities arise from this approach, and one method of removing them which seems to work well for identical particles is presented. Removal of these singularities forces a reconsideration of the size of the three body forces, and the new estimates give somewhat smaller results than those obtained in Sec. III.

A. Relativistic fully-off-shell Faddeev equations

Using diagrams, we first review how a set of three body relativistic integral equations of the Faddeev type can be constructed. Since all three particles are first allowed to be off their mass shell, the three body Green's functions depend here on two relative four-momenta. Our underlying dynamical assumption is that a satisfactory approximation to the relativistic three body scattering amplitude \mathcal{M} is the infinite sum of all ladder and crossed ladder diagrams due to the exchange of scalar mesons. Instead of trying to sum these directly, it is customary to construct an integral equation which will reproduce the sum when iterated and will ensure that the result is unitary. The solution of the equation is regarded as the physical content of the infinite sum and will exist even when the sum diverges.

For the three body problem, following the Faddeev approach, we construct a set of coupled equations for some partial amplitudes, each of these amplitudes corresponding to the separate summation of a subclass of three-body diagrams. We introduce the set of partial amplitudes \mathcal{T}^i and \mathcal{T}^0 such that

$$\mathcal{M} = \sum_i \mathcal{T}^i + \mathcal{T}^0. \tag{1.1}$$

(See Fig. 1.) This set will be referred to collectively as \mathcal{T}^α (Greek indices run from 0 to 3, Latin indices from 1 to 3). The amplitude \mathcal{T}^i will contain all diagrams where particle i does not interact in the last part (left) of the diagram (i.e., where particle i ends as a spectator) while \mathcal{T}^0 will contain all diagrams in which the last part is three body irreducible (i.e., where the last part of the interaction can be defined as a three body force). Inspection of the structure

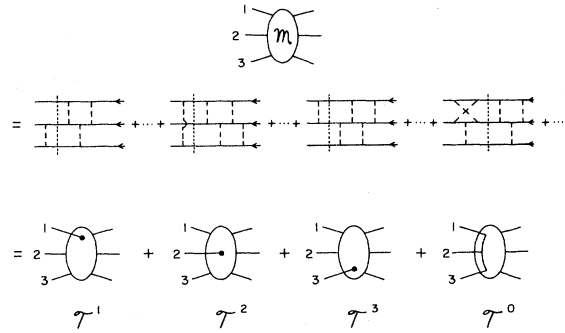


FIG. 1. A small sample of the sum of ladder and crossed ladder diagrams showing how the partial amplitudes \mathcal{T}^α arise naturally.

of the diagrams of one particular subclass (this is done for \mathcal{T}^3 in Fig. 2) immediately suggests an integral equation for this partial amplitude, in which the two body scattering amplitude M^i (where i is the index of the noninteracting particle) emerges as a driving term from the gathering of all the disconnected parts that are singled out at the end of each diagram. The other partial amplitudes will obey similar equations so that we obtain a set of four coupled integral equations. In the \mathcal{T}^0 equation, the driving term is \mathcal{Y}^0 , constructed by iteration of all three-body irreducible diagrams (whose sum is represented by \mathcal{X}^0). We call this new driving term the three body unitarized force (TUF). This is illustrated in Fig. 3. Diagrams which contribute to the irreducible three body force will be given in Sec. III.

These relativistic, fully off shell equations are deceptively simple in appearance. They are actually quite complicated because as they stand, the three body Green's function depends on eight variables, the components of two relative four-momenta. The similar nonrelativistic theory depends on only six variables. Several approaches have been developed which eliminate the additional two variables (relative energies) in a completely covariant way.^{1,3,4} To

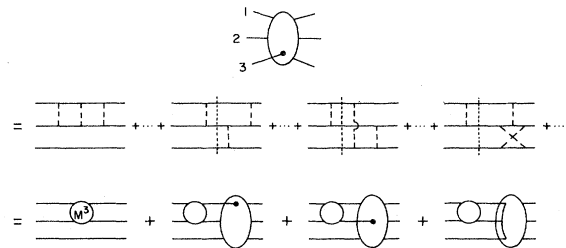


FIG. 2. Illustration of how the equation for \mathcal{T}^3 arises from the sum of ladder and crossed ladder diagrams:

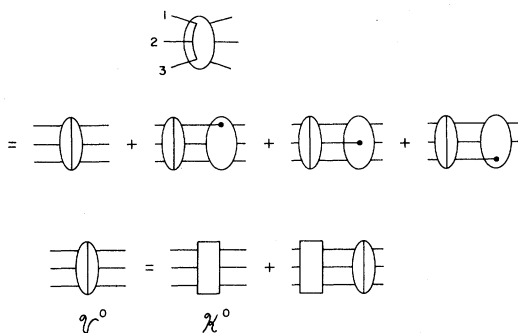


FIG. 3. Diagrammatic representation of the equations for \mathcal{S}^0 and the γ^0 .

motivate the procedure introduced in this paper requires that we return to the original sum of ladder and crossed ladder diagrams and look at the same dynamics from a different point of view.

B. Relativistic Faddeev equations with one particle off shell

We begin by looking at the simplest diagrams that are of significance in the three body problem, i.e., those of the sixth order. There are three basic types (to which we must add the permutations having the same topology) shown in Figs. 4 and 5. The first type, in Fig. 4, can be separated into two disconnected pieces by one three body cut. Across this cut, one of the nucleons is interacting while the other two are spectators; later, our analysis will suggest that we put these spectators on their mass shell which will make these diagrams have a structure comparable to the pole diagram shown in Fig. 4(b) in which the amplitudes are directly related to those introduced in I. Hence we may regard these diagrams of the first type as an iteration of the two-body force and they will make no contribution to the three-body force.

The other two basic types of sixth order diagrams are shown in Fig. 5. Those shown in Figs. 5(a) and (b) can be separated into a connected and a disconnected piece while those in Figs. 5(c) and (d) cannot be reduced at all (of course in higher order there are many diagrams that can be reduced into two connected pieces). The latter are clearly part of the three body force while the former will be separated into two parts. One part is designed to be obtained from the iteration of two-body amplitudes like the diagrams of the first type (Fig. 4) while the other part will be included in the three body force.

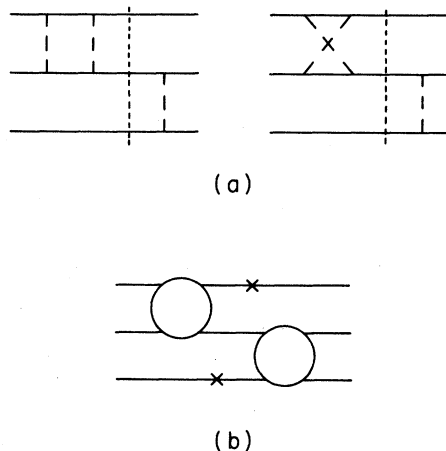


FIG. 4. (a) Sample diagrams which can be cut into two disconnected pieces, with one three body cut. (b) Representation of the sum of such diagrams. The \times 's always represent a particle on mass shell.

The way in which the diagrams 5(a) and (b) are separated into two pieces is the major idea of this paper. Before discussing this in detail, we take a broad look at the physics of the three body problem.

A central idea in any Faddeev theory of three particles scattering without large three body forces is that most of the effective three body force is generated by a succession of two body scattering. In order for this to be true, it must be true that the diagrams in Figs. 5(a) and (b) dominate over the corresponding diagrams in Figs. 5(c) and (d). This is indeed the case at low energies where this dominance is often understood in terms of unitarity cuts. The first two cases have elastic three-body cuts with a threshold at $9M^2$, while the next two have no elastic cut, and a correspondingly higher threshold at $(3M + \mu)^2$.

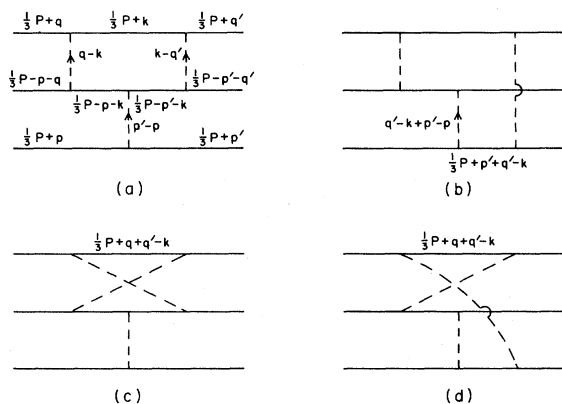


FIG. 5. Four representative diagrams discussed in the text.

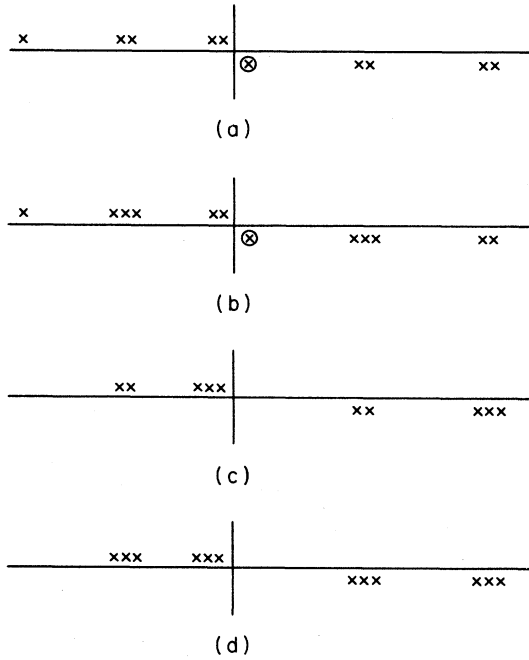


FIG. 6. Location of the singularities in the complex k_0 plane for the four diagrams shown in Fig. 5.

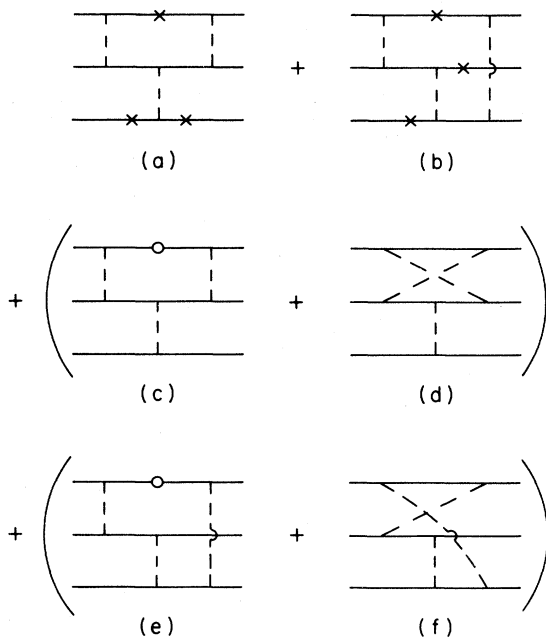


FIG. 7. Separation of the diagrams of Fig. 5 into parts which are reducible (a) and (b), and parts which are irreducible (c) through (f) and destined to be included in the three body force.

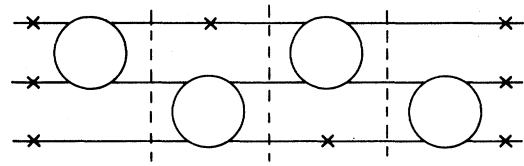


FIG. 8. Successive interactions involving the pairs (1,2) and (2,3) with the spectators put on shell (marked with an \times). Examination of the cuts shows how the requirement that two particles are always on shell comes about.

In terms of the ideas presented in I, the dominance of the first two diagrams over the latter two is understood in terms of the location of singularities in the complex k_0 plane, where k_0 is the virtual loop energy, labeled in Fig. 5 for each of the diagrams. There are 10 poles in the k_0 plane for Figs. 5(a) and (c) and 12 poles for 5(b) and (d) corresponding to the positive and negative energy poles of the nucleon and meson propagators. The location of these singularities is shown schematically in Fig. 6 for the four diagrams. Note that if we close the k_0 contour in the lower half-plane, Figs. 5(a) and (b) are dominated by the contribution from the nucleon pole close to $k_0=0$ (shown circled in the figures). This is because the residue of the integrand at this pole will be quite large because of its proximity to the two other nucleon poles in the upper half-plane also near $k_0=0$. Furthermore, the dominant piece of these diagrams has a direct physical interpretation; it corresponds to placing the "spectator" nucleon of the loop on its mass shell. Hence we have a very nice physical result. The dominant parts of Figs. 5(a) and (b) come from that part of the interaction where the spectator is a physical on shell particle. In Figs. 5(c) and (d) where there is no spectator there are also no such poles to dominate and this explains why these contributions are much smaller than the reducible ones.

The next step is to separate out the leading pole contribution from the reducible diagram and lump the remaining contributions from the other poles with the irreducible diagram. This decomposition and rearrangement of terms is illustrated in Fig. 7. In the first two diagrams, the spectator is on shell and these leading contributions will be included in the iteration of successive two body scatterings implied by the Faddeev equation. The last four terms will be taken together and constitute a new definition of the irreducible part of the three body interaction, i.e., of the intrinsic three body force.

The above discussion can be extended to interac-

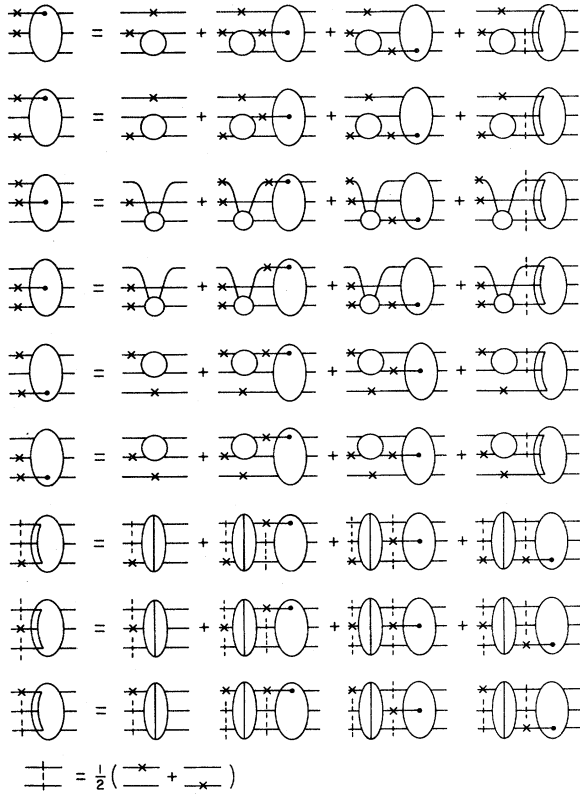


FIG. 9. Diagrammatic representation of the 12 coupled equations discussed in the text. Mass shell particles are marked with an \times . When they are associated with internal particles, the vertical dashed lines represent the average of the two possible choices for on shell particles. With external particles they represent two equations for the two possibilities. The \times on all TUF's and \mathcal{T}^0 's also represents the spectator.

tions of all orders, i.e., one can always find a labeling of the loop momentum which will show that the dominant energy singularity occurs when the spectator particle is on shell. When there are a series of interactions as shown in Fig. 8, placing the spectator on shell will ultimately force *two* of the particles to be on shell, uniquely defining the Green's function. We then separate out all of these dominant terms to be summed as a succession of two body interactions and incorporate the remaining terms into the three body force. This force now includes a huge number of parts, some of which would be present in the original formalism sketched in Sec. A, and others which are pieces of Feynman diagrams left over from our separation. In Sec. III we will discuss this point in considerably more detail.

The systematic placing of spectators on the mass

shell will force us to use a larger set of amplitudes in order to maintain the completeness of our set of coupled equations and to have everywhere two-body driving terms of the type developed in I, i.e., with one initial and one final particle on shell. We deal with amplitudes obtained from \mathcal{T}^α by putting two of their final particles on shell. For \mathcal{T}^i the spectator and one of the final interacting particles are on shell; we denote these amplitudes by \mathcal{T}_j^i , where $i = 1, 2, 3$ is the spectator and $j = 1, 2, 3 \neq i$ is the interacting particle which is kept off shell. There are a total of six of these. For the \mathcal{T}^0 amplitude there would appear to be no spectator, yet we will find in Sec. III that our method of separating out the three body force sometimes generates terms in which a particular particle is favored as the spectator. We find it necessary to introduce six amplitudes $\mathcal{T}_j^0(i)$, where $j \neq i$ is the off shell particle and i is again the spectator. Amplitudes in which no particular choice of j or i is preferred will contribute equally to all $\mathcal{T}_j^0(i)$, while others will contribute more to one than another. (Since the choice of spectator i is clear from the structure of the equation, it will normally be suppressed.) In the equation for the amplitude \mathcal{T}_j^i , there are two possible choices of j' in the \mathcal{T}_j^0 terms, and both terms are included (multiplied by $\frac{1}{2}$). Similarly, in the equations for \mathcal{T}_j^0 there are two choices of j' in the \mathcal{T}_j^i terms, and we again take one half the sum of both. These symmetric choices, together with the full set of six \mathcal{T}_j^0 , actually simplifies the mathematical notation in Sec. II, and, to the extent that the amplitudes differ from one another, is required by unitarity.

The final set of three-body equations, illustrated in Fig. 9, is a coupled set of 12 equations for the 12 amplitudes \mathcal{T}_j^α ($j \neq \alpha$) driven by 45 terms $\mathcal{V}_{jj'}^\alpha$, where j' denotes the off shell particle in the initial state (and the dependence of \mathcal{T}^0 on i and i' has been suppressed). The $\mathcal{V}_{jj'}^\alpha$ can be expressed in terms of the set of off shell two body amplitudes $M_{jj'}^i$ introduced in I. The three body driving terms $\mathcal{V}_{jj'}^\alpha$ are obtained by unitarizing the three body irreducible kernel, which is composed of diagrams of the type shown in Figs. 7(c)–(f). Of these, only diagrams (d) and (f) would have been present in a Bethe-Salpeter formalism; the other two, (c) and (e), are pieces which we pick up from the decomposition discussed above.

Although the final set of 12 equations illustrated diagrammatically in Fig. 9 looks more complicated than the set given in subsection A, it may actually be simpler because the integration over the intermediate Green's functions is now six dimensional. Furthermore, for three identical particles, there are

relations between the amplitudes which reduce the system back to only four independent coupled equations.

Perhaps the most appealing feature of this formalism is that it is very intimately connected to the fundamental dynamics suggested by the sum of ladder and crossed ladder diagrams. The two body driving terms are known and the three body driving terms can be calculated in precisely the same approximation one finds satisfactory for two-body problems.

II. MATHEMATICAL PROPERTIES OF THE EQUATIONS

In this section, the diagrams of the previous section will be converted into algebraic equations. The two body amplitudes which drive the equations will be discussed, and it will be shown that they are precisely those obtained in I, hence the cluster property is satisfied. Three body unitarity will be proved.

A. The three body Green's function

The three particles have masses M_1 , M_2 , and M_3 , and four-momenta p_1 , p_2 , p_3 (denoted collectively as $\{p\}$) which are constrained by energy momentum conservation

$$P = p_1 + p_2 + p_3. \quad (2.1)$$

As independent variables we will often choose one of the p_i (the spectator) and the relative momentum of the other two, as discussed below.

Three different three body Green's functions are needed. For spinless particles they are

$$G_j(\{p\}) = (2\pi)^2 \frac{\delta_+(M_i^2 - p_i^2) \delta_+(M_k^2 - p_k^2)}{[M_j^2 - p_j^2 - i\epsilon]} \\ = (2\pi) \delta_+(M_i^2 - p_i^2) G_j^{(2)}(\{p\}), \quad (2.2)$$

where $G^{(2)}$ is the two body Green's function used in I, j will always denote the particle which is *off shell*, and i and k ($i \neq k$ and both not equal to j) denote the on shell particles. Equation (2.2) is really the kernel of an integral operator, where we will use the notation

$$\Sigma = \int \frac{d^4 p_k d^4 p_i}{(2\pi)^8} \\ = \int \frac{d^4 p_i}{(2\pi)^4} \Sigma^{(2)}. \quad (2.3)$$

Any independent pair of momenta can be used in (2.3). Note that (2.2) and (2.3) are manifestly covariant.

The δ_+ functions in (2.2) fix the fourth components of p_i and p_k

$$p_{i0} = E_i = (M_i^2 + \vec{p}_i^2)^{1/2}, \\ p_{k0} = E_k = (M_k^2 + \vec{p}_k^2)^{1/2}, \quad (2.4)$$

leaving only six momentum variables in the Green's function.

B. Two body driving terms and the cluster property

When working with the two body amplitudes M^i (introduced in Sec. I), it is convenient to introduce new variables in place of the momenta p_j and p_k . These will be the total momentum and the relative momentum of the interacting pair, defined according to

$$P_i = p_j + p_k, \\ Q_{ij} = \frac{1}{2}(p_k - p_j). \quad (2.5)$$

Note that the relative momentum depends on which of the two interacting particles is on shell, and that in our notation

$$\vec{Q}_{ij} = -\vec{Q}_{ik}. \quad (2.6)$$

The two body driving terms in the three body space can be written

$$\mathcal{V}_{jj'}^i(p_i Q_{ij} Q'_{ij'}) = (2\pi)^3 2E_i \delta^3(p_i - p'_i) \\ \times M_{jj'}^i(P_i Q_{ij} Q'_{ij'}), \quad (2.7)$$

where the covariant form of the three dimensional δ function has been used.

We will now show that the two body amplitudes M^i satisfy the two body equation discussed in I. To this end, recall that, in the context of three body theory, the disconnected two body driving terms (2.7) arise from the iteration of the elementary irreducible two body kernels, as shown in Fig. 10 in the one pion exchange (OPE) approximation. These elementary kernels will be written

$$\mathcal{X}_{jj'}^i(p_i Q_{ij} Q'_{ij'}) = (2\pi)^3 2E_i \delta^3(p_i - p'_i) \\ \times V_{jj'}^i(P_i Q_{ij} Q'_{ij'}), \quad (2.8)$$

where for exchange of a particle of mass μ ,

$$V_{jj'}^i(P_i Q_{ij} Q'_{ij'}) = [\mu^2 - t_i(j, j')]^{-1} \quad (2.9)$$

and the square of the momentum transfer is

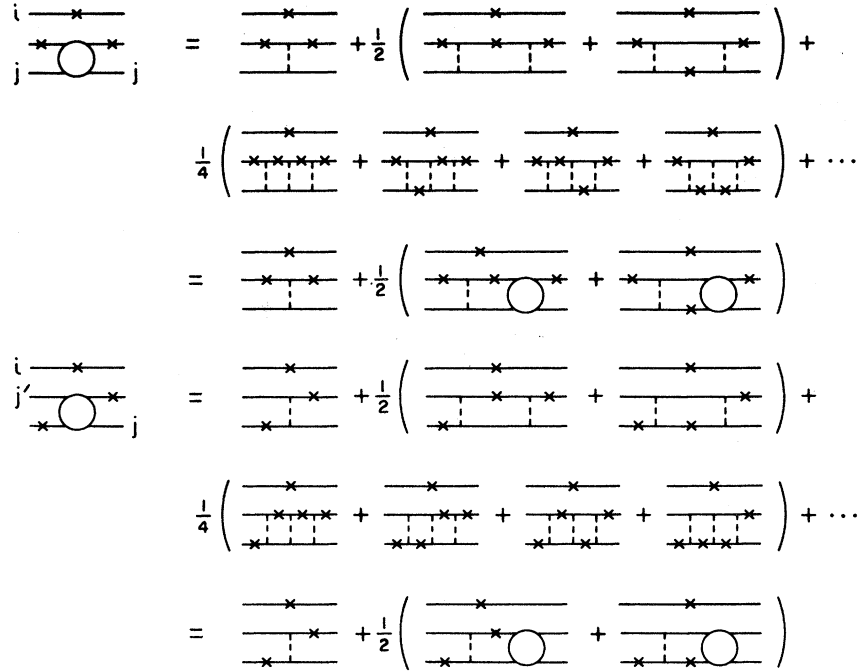


FIG. 10. Illustration of the origin of the symmetric two body equations with one particle on shell.

$$t_i(j, j') = \begin{cases} (Q_{ij} - Q'_{ij})^2 = (E_k - E'_k)^2 - (\vec{Q}_{ij} - \vec{Q}'_{ij})^2 & j' = j, \\ (Q_{ij} + Q'_{ik})^2 = (E_k + E'_j - P_i)^2 - (\vec{Q}_{ij} + \vec{Q}_{ik})^2 & j' = k. \end{cases} \quad (2.10)$$

The equation satisfied by $\mathcal{Y}^i_{jj'}$ is

$$\begin{aligned} \mathcal{Y}^i_{jj''}(p_i Q_{ij} Q_{ij''}) &= \mathcal{X}^i_{jj''}(p_i Q_{ij} Q_{ij''}) \\ &\quad - \frac{1}{2} \sum_{j'} \mathcal{X}^i_{jj'}(p_i Q_{ij} Q_{ij'}) G_{j'}(\{p'\}) \mathcal{Y}^i_{j'j''}(p_i Q_{ij'} Q_{ij''}), \end{aligned} \quad (2.11)$$

where the symmetric sum over the choice of off shell particles, j' , has been written explicitly. Performing the integrations over p_i , and dropping common factors on both sides of (2.11) gives an equation for $M^i_{jj'}$

$$\begin{aligned} M^i_{jj''}(P_i Q_{ij} Q_{ij''}) &= V^i_{jj''}(P_i Q_{ij} Q_{ij''}) \\ &\quad - \frac{1}{2} \sum_{j'}^{(2)} V^i_{jj'}(P_i Q_{ij} Q_{ij'}) G^{(2)}(\{p'\}) M^i_{j'j''}(P_i Q_{ij'} Q_{ij''}). \end{aligned} \quad (2.12)$$

This equation is manifestly covariant, and is a symmetrized version of the form given in I. [Since the three body equations require both j 's, unitarity requires the symmetrized version of (2.12) also; the equation is also unitary if only one of j appears everywhere.] The only way in which (2.12) is affected by the presence of the spectator is through the total four-momentum of the two body system.

Hence the two body amplitudes used in the three body problem are identical with those used in the two body problem, and the cluster property is established. It should be noted, however, that the integration over p_i will force p_i^2 to negative values, requiring that the two body equations be solved for both timelike and spacelike regions.

C. The three body equations

This section describes in detail how the variables are introduced into the equations, and a compact mathematical expression obtained.

The partial amplitudes \mathcal{S}_j^i will always carry the choice p_i, Q_{ij} for their arguments

$$\mathcal{S}_j^i = \mathcal{S}_j^i(p_i Q_{ij}; \{p'\}), \quad (2.13)$$

where $\{p'\}$ denotes the arguments of the initial state. There are six of these amplitudes ($i \neq j$). The six three body terms $\mathcal{S}_j^i(i)$ will be written:

$$\mathcal{S}_j^0 = \mathcal{S}_j^0(p_i Q_{ij}; \{p'\}). \quad (2.14)$$

To satisfy unitarity, it is necessary to use all possible choices of (2.14) in a symmetric way just as for the two body amplitudes discussed above. Every

one of the \mathcal{S}^0 amplitudes will occur exactly twice in the first six equations, and each of the amplitudes (2.13) occurs exactly once in each of the last six equations.

There are a total of $6 \times 6 = 36$ different choices possible for the TUF driving term

$$\mathcal{Y}_{jj'}^0 = \mathcal{Y}_{jj'}^0(p_i Q_{ij}; p_{i'} Q_{i'j'}). \quad (2.15)$$

All 36 of these enter into the last six equations in Fig. 9 precisely once, and 12 of them are also needed in the first six equations.

The 12 equations of Fig. 9 can now be written in a compact form. We will enlarge the set by allowing the initial state to be off shell also, although no particular choice of the initial momenta $\{p'\}$ will be specified. Thus finally

$$\begin{aligned} \mathcal{T}_{jj'}^{\alpha\alpha'}(p_i Q_{ij}; \{p'\}) &= \delta_{\alpha\alpha'} \mathcal{Y}_{jj'}^\alpha(p_i Q_{ij}; \{p'\}) \\ &- \sum_{\alpha_1 j_1} \theta_{\alpha\alpha_1 j_1} \mathcal{Y}_{jj_1}^\alpha(p_i Q_{ij}; \tilde{p}_{i'} \tilde{Q}_{i'j'}) G_{j_1}(\{\tilde{p}\}) \mathcal{T}_{j_1 j'}^{\alpha_1 \alpha'}(\tilde{p}_{i'} \tilde{Q}_{i'j'}; \{p'\}), \end{aligned} \quad (2.16a)$$

where

$$\begin{aligned} \sum_{\alpha_1 j_1} \theta_{\alpha\alpha_1 j_1} &= \sum_{\alpha_1 j_1} \int \frac{d^4 \tilde{p}_{i'} d^4 \tilde{Q}_{i'j_1}}{(2\pi)^8} (1 - \delta_{\alpha\alpha_1})(1 - \delta_{\alpha_1 j_1})(1 - \delta_{\alpha j_1}) \xi_{\alpha_1} \xi_\alpha \\ \xi_\alpha &= \begin{cases} 1 & \alpha \neq 0, \\ \frac{1}{2} & \alpha = 0. \end{cases} \end{aligned} \quad (2.17)$$

Any indices involved in (2.17) will always be written explicitly on the summation sign, which by itself will denote the two four-dimensional integrals only. Note that, for fixed α', j' , and $\{p'\}$, (2.16a) gives the expected 12 equations. If $\alpha \neq 0$, then α must equal i (the spectator) and for each i there are two choices of j , giving six equations. When $\alpha = 0$, there are six possible choices of $j \neq i$. The θ term in the sum ensures that precisely the correct terms are present. It gives use the requirement that $\alpha_1 \neq \alpha$, required by the definitions. When both α_1 and α are not zero, this gives precisely one term, and $i' = \alpha_1$. When either α_1 or α is zero, we have two terms, multiplied by $\frac{1}{2}$ as required by the symmetry. For the case $\alpha \neq 0, \alpha_1 = 0$, the driving term fixes $i' = i$. When $\alpha = 0, \alpha_1 \neq 0$, the \mathcal{T} term fixes $i' = \alpha_1$. In no case must the sum over i' be considered, and we can drop all reference to it, along with the arguments, which are uniquely specified by the rules and notation we have introduced. This gives

$$\begin{aligned} \mathcal{T}_{jj'}^{\alpha\alpha'} &= \delta_{\alpha\alpha'} \mathcal{Y}_{jj'}^\alpha \\ &- \sum_{\alpha_1 j_1} \theta_{\alpha\alpha_1 j_1} \mathcal{Y}_{jj_1}^\alpha G_{j_1} \mathcal{T}_{j_1 j'}^{\alpha_1 \alpha'}. \end{aligned} \quad (2.16b)$$

Similarly, by iterating the driving terms from the left, we have

$$\begin{aligned} \mathcal{T}_{jj'}^{\alpha\alpha'} &= \delta_{\alpha\alpha'} \mathcal{Y}_{jj'}^{\alpha'} \\ &- \sum_{\alpha_1 j_1} \theta_{\alpha_1 \alpha' j_1} \mathcal{T}_{jj_1}^{\alpha\alpha_1} G_{j_1} \mathcal{Y}_{j_1 j'}^{\alpha'}. \end{aligned} \quad (2.18)$$

D. Unitarity of the driving terms

The driving terms all satisfy the equation

$$\mathcal{Y}_{jj'}^\alpha = \mathcal{X}_{jj'}^\alpha - \eta_\alpha \sum_{j_1} \mathcal{X}_{jj_1}^\alpha G_{j_1} \mathcal{Y}_{j_1 j'}^\alpha, \quad (2.19)$$

where the sum over j_1 includes all possible choices

of spectator and

$$\eta_\alpha = \begin{cases} \frac{1}{2} & \alpha \neq 0 \\ \frac{1}{3} & \alpha = 0 \end{cases}$$

assures that there is no overcounting by dividing by the number of terms in the symmetric sum. In (2.19) the two different choices of spectator possible when $\alpha = 0$ have been collected into one term by

labeling the momenta, otherwise $\eta_0 = \frac{1}{6}$. The kernels \mathcal{K}^i were defined in (2.8) and \mathcal{K}^0 is the sum of all irreducible three body kernels, and is defined just as in (2.15). Similarly, for all α

$$\mathcal{Y}_{jj'}^\alpha = \mathcal{K}_{jj'}^\alpha - \eta_\alpha \sum_{j_1} \mathcal{Y}_{jj_1}^\alpha G_{j_1} \mathcal{K}_{j_1 j'}^\alpha. \quad (2.20)$$

We will now prove that these driving terms are unitary. Taking the complex conjugation of (2.20) and multiplying from the right by $G\mathcal{Y}$ and integrating and summing gives

$$\eta_\alpha \sum_{j_1} \mathcal{Y}_{jj_1}^{\alpha*} G_{j_1} \mathcal{Y}_{j_1 j'}^\alpha = \eta_\alpha \sum_{j_1} \mathcal{K}_{jj_1}^\alpha G_{j_1} \mathcal{Y}_{j_1 j'}^\alpha - \eta_\alpha^2 \sum_{j_1 j_2} \mathcal{Y}_{jj_1}^{\alpha*} G_{j_1}^* \mathcal{K}_{j_1 j_2}^\alpha G_{j_2} \mathcal{Y}_{j_2 j'}^\alpha, \quad (2.21)$$

where we assumed \mathcal{K}^α was real (below the production thresholds). Multiplying (2.19) from the left by $\mathcal{Y}^* G^*$ and integrating gives a similar equation

$$\eta_\alpha \sum_{j_1} \mathcal{Y}_{jj_1}^{\alpha*} G_{j_1} \mathcal{Y}_{j_1 j'}^\alpha = \eta_\alpha \sum_{j_1} \mathcal{K}_{jj_1}^\alpha G_{j_1} \mathcal{Y}_{j_1 j'}^\alpha - \eta_\alpha^2 \sum_{j_1 j_2} \mathcal{Y}_{jj_1}^{\alpha*} G_{j_1}^* \mathcal{K}_{j_1 j_2}^\alpha G_{j_2} \mathcal{Y}_{j_2 j'}^\alpha, \quad (2.22)$$

Use the equations (2.19) and (2.20) to reduce the first term on the right-hand side of each equation, and note that the second term on the right-hand side is identical in both equations. Subtracting the two equations gives:

$$\mathcal{Y}_{jj'}^{\alpha*} - \mathcal{Y}_{jj'}^\alpha = -\eta_\alpha \sum_{j_1} \mathcal{Y}_{jj_1}^{\alpha*} [G_{j_1}^* - G_{j_1}] \mathcal{Y}_{j_1 j'}^\alpha. \quad (2.23)$$

The discontinuity of the three body Green's function (2.2) is

$$\begin{aligned} G_{j_1}^* - G_{j_1} &= -(2\pi)^3 i \delta_+ [M_1^2 - p_1^2] \delta_+ [M_2^2 - p_2^2] \delta_+ [M_3^2 - p_3^2] \\ &\equiv \delta_0, \end{aligned} \quad (2.24)$$

which is the integrand of the three body phase space integral and which is clearly independent of j_1 . Hence the j_1 sum is trivial, and cancels the η_α factor giving

$$\mathcal{Y}_{jj'}^{\alpha*} - \mathcal{Y}_{jj'}^\alpha = -\sum \mathcal{Y}_{j_0}^{\alpha*} \delta_0 \mathcal{Y}_{0j'}^\alpha, \quad (2.25)$$

where the subscript 0 on \mathcal{Y} reminds us that the state has all three particles on shell, and hence does not depend on j_1 . Explicitly:

$$\begin{aligned} \text{Im} \mathcal{Y}_{jj'}^\alpha &= -\pi \int \frac{d^4 \tilde{p}_1 d^4 \tilde{p}_2}{(2\pi)^6} \mathcal{Y}_{j_0}^{\alpha*} \delta_+ [M_1^2 - \tilde{p}_1^2] \delta_+ [M_2^2 - \tilde{p}_2^2] \delta_+ [M_3^2 - \tilde{p}_3^2] \mathcal{Y}_{0j'}^\alpha \\ &= -\pi \int \frac{d^3 \tilde{p}_1 d^3 \tilde{p}_2 \delta(W - E_1 - E_2 - E_3)}{(2\pi)^6 8E_1 E_2 E_3} \mathcal{Y}_{j_0}^{\alpha*} \mathcal{Y}_{0j'}^\alpha. \end{aligned} \quad (2.26)$$

For the two body driving terms, we can use (2.7) to reduce this result further

$$\text{Im} M_{jj'}^i = -\pi \int \frac{d^3 Q_i \delta(P_{i0} - E_j - E_k)}{(2\pi)^3 4E_j E_k} M_{j_0}^{i*} M_{0j'}^i, \quad (2.27)$$

which is a familiar result for two body unitarity.

E. Unitarity of the full three body amplitude

The unitarity of the driving terms will now be used to establish three body elastic unitarity of the full three body amplitude (1.1). The proof repeats the argument used in the last section, but is slightly more complicated because the driving terms are now complex. If we repeat the same steps used before, but apply them to Eqs. (2.16b) and (2.18), we obtain for the analog to (2.23)

$$\begin{aligned} \sum_{\substack{\alpha_1 j_1 \\ \alpha_2}} \mathcal{T}_{jj_1}^{\alpha\alpha^*} \theta_{\alpha_1 \alpha_2 j_1} [G_{j_1}^* - G_{j_1}] \mathcal{T}_{j_1 j'}^{\alpha_2 \alpha'} = & - \sum_{\alpha_1 j_1 \alpha_2 j_2 \alpha''} \mathcal{T}_{jj_1}^{\alpha\alpha^*} G_{j_1}^* \theta_{\alpha_1 \alpha'' j_1} [\mathcal{Y}_{j_1 j_2}^{\alpha''} - \mathcal{Y}_{j_1 j_2}^{\alpha''*}] \theta_{\alpha'' \alpha_2 j_2} G_{j_2} \mathcal{T}_{j_2 j'}^{\alpha_2 \alpha'} \\ & + \sum_{\alpha_1 j_1} \mathcal{T}_{jj_1}^{\alpha\alpha^*} G_{j_1}^* \theta_{\alpha' \alpha_1 j_1} \mathcal{Y}_{j_1 j'}^{\alpha'} - \sum_{\alpha_1 j_1} \mathcal{Y}_{jj_1}^{\alpha^*} G_{j_1} \theta_{\alpha_1 \alpha j_1} \mathcal{T}_{j_1 j'}^{\alpha_1 \alpha'}, \end{aligned} \quad (2.28)$$

where the symmetry of θ in its first two indices was used. The unitary relation (2.25) is now used to replace the discontinuity of \mathcal{Y} with $\mathcal{Y}^* \mathcal{Y}$ in the first term on the right-hand side, and in the last two terms \mathcal{Y} and \mathcal{Y}^* can be changed to \mathcal{Y}^* and \mathcal{Y} . Then Eqs. (2.16b) and (2.18) are used repeatedly to reduce and cancel terms. The result is

$$\begin{aligned} \mathcal{T}_{jj'}^{\alpha\alpha^*} - \mathcal{T}_{jj'}^{\alpha\alpha'} = & - \sum_{\alpha''} \mathcal{T}_{j_0}^{\alpha\alpha''*} \delta_0 \mathcal{T}_{0j'}^{\alpha''\alpha'} \\ & - \sum_{\alpha_1 j_1 \alpha_2} \mathcal{T}_{jj_1}^{\alpha\alpha^*} \theta_{\alpha_1 \alpha_2 j_1} \delta_0 \mathcal{T}_{j_1 j'}^{\alpha_2 \alpha'}. \end{aligned} \quad (2.29)$$

The last term no longer depends on j_1 except through θ . We see that if α_1 and α_2 are both not equal to zero, there is only one term in the j_1 sum. If either α_1 or α_2 is zero, there are two terms, which cancels the $\frac{1}{2}$ from the factor of θ . Hence, the last term reduces to

$$- \sum_{\substack{\alpha_1 \\ \alpha_2 \neq \alpha_1}} \mathcal{T}_{j_0}^{\alpha\alpha^*} \delta_0 \mathcal{T}_{0j'}^{\alpha_2 \alpha'}.$$

When the diagonal terms from the first term on the right-hand side are included, we obtain the three body unitary relation

$$\begin{aligned} \mathcal{T}_{jj'}^{\alpha\alpha^*} - \mathcal{T}_{jj'}^{\alpha\alpha'} = & - \sum \left[\sum_{\alpha_1} \mathcal{T}_{j_0}^{\alpha\alpha_1} \right] \\ & \times \delta_0 \left[\sum_{\alpha_2} \mathcal{T}_{0j'}^{\alpha_2 \alpha'} \right], \end{aligned} \quad (2.30)$$

where the terms in parentheses are just the full three body amplitude (1.1) for the case when the intermediate states are physical, where only the α label distinguishes the partial amplitudes from each other.

III. THREE BODY FORCES

In this section the three body forces which appear in a simple theory involving scalar particle exchange will be described and estimated.

A. Contributions to the sixth order irreducible kernel

The first contributions to the three body force in this simple theory come from sixth order exchange, as described already in Sec. I. The diagrams were shown in Fig. 7(c)–(f) and will be referred to as diagrams of type *A*, *B*, *C*, or *D*, respectively.

If the heavy particles (nucleons) are not identical, but the light mesons are, then there are 20 distinct diagrams which include six of type *A*, *B*, and *C*, but only two of type *D*, all shown in Fig. 11. To see how they distribute themselves among the various three body driving terms, we consider the iteration of the system of equations illustrated in Fig. 9. To lowest order, TUF may be replaced by \mathcal{X}^0 , and there are 36 different \mathcal{X}^0 's. Certain of the three body terms shown in Fig. 11 must always be associated with cases in which a particular particle in the initial and final state is on shell. These are the terms of type *A* and *C*, and the favored particles,

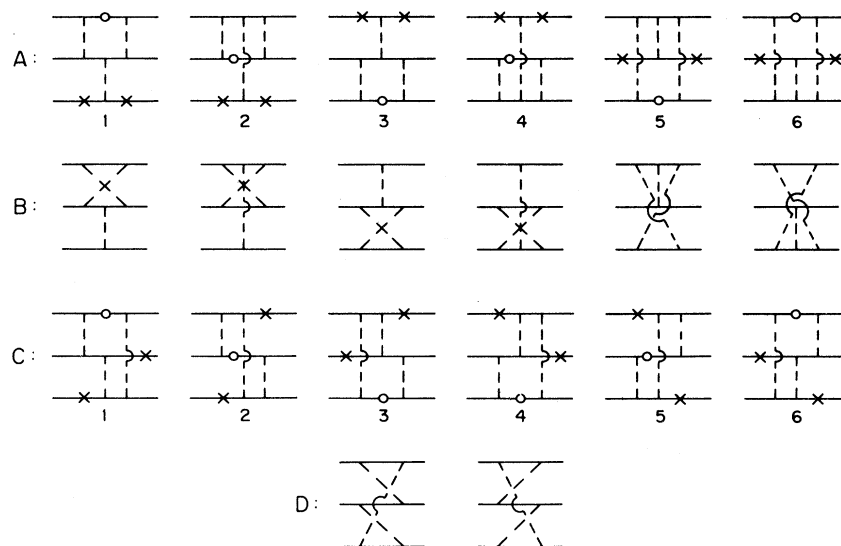


FIG. 11. The 20 three body driving terms which contribute to the sixth order three body kernel.

which must be on shell, are marked in the figure. The origin of these restrictions can be understood by considering such a diagram in conjunction with all possible OPE interactions, both before and after. As a simple example of how this works, Fig. 12 shows the origin of the final state restriction for the amplitude A_1 , which arises from contributions neglected when particle 1 was put on shell as shown in the diagram. (The contributions neglected when particle 3 is put on shell give rise to other three body, or higher, forces not shown in the figure.) The figure shows that no matter which pair is involved in the interaction subsequent to A_1 , particle 3 will always be the final state spectator and must therefore be on shell whenever A_1 is used. The same analysis explains the origin of both the final state and initial state restrictions on all the diagrams of type *A* and *C*.

While it may appear that particle 3 is also a spectator for the first diagram of type *B* shown in Fig. 11, examination of the singularities of the diagram (recall Fig. 6) shows that the internal nucleon poles are always distant from the external nucleon poles, so that there is no pinch between particle 3 and any of the internal particles and therefore no reason to prefer particle 3 as a spectator. All of the diagrams of type *B* and *D* show this property.

The composition of each of the 36 elementary kernels can now be constructed with the help of Fig. 11. We denote the kernels by $\mathcal{K}_{jj'}^0(i, i')$, where j and j' are the off shell particles and i, i' are the spectator particles. Care must be taken to give the

correct weight to each of the diagrams. Of course, no diagram which requires the j th final state particle, or the j' th initial state particle, to be on shell can contribute to $\mathcal{K}_{jj'}^0(i, i')$. Furthermore, it must be remembered that the equations are defined so that when iterated the kernels appear in symmetrized combinations like

$$\frac{1}{4} \sum_{j_1 \neq i} \sum_{j_2 \neq i'} \mathcal{V}_{jj_1}^i \mathcal{K}_{j_1 j_2}^0(i, i') \mathcal{V}_{j_2 j'}^{i'}, \quad (3.1)$$

where the Green's functions have been omitted from (3.1). These usually appear naturally by taking one-half of the two possible choices of the off shell particle in both the initial and final states. In this case, the diagram contributes to all four terms in the sum (3.1). However, for diagrams of type *A* and *C* an unsymmetric choice is sometimes required

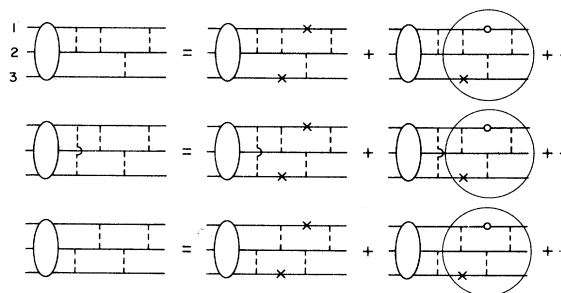


FIG. 12. Diagrams illustrating how it comes about that diagram A_1 of Fig. 11 must always have particle 3 on shell.

by spectator rules, in which case if only one j is permitted in *either* the initial *or* the final state, the diagram must be multiplied by 2 to reflect the fact that it can contribute to only two terms in the sum (3.1). When only one j is permitted in *both* the initial *and* final state, the full diagram contributes to only one term and must be multiplied by 4 in order that its full weight be counted.

The structure of six kernels \mathcal{K}^0 will now be given. In each case, *all* diagrams of type B and D contribute. The additional ones of type A and C included in each case are the following:

$$\begin{aligned}\mathcal{K}_{22}^0(1,1) &: 4A_1 + 4A_2 + A_3 + A_4 + 2C_2 + 2C_5, \\ \mathcal{K}_{22}^0(3,1) &: 2A_1 + 2A_2 + 2A_3 + 2A_4 + C_2 + 4C_5, \\ \mathcal{K}_{12}^0(3,1) &: 2A_1 + 2A_2 + C_2 + 2C_3 + 4C_6, \\ \mathcal{K}_{12}^0(2,1) &: 4A_1 + 4A_2 + 2C_2 + C_3 + 2C_6, \\ \mathcal{K}_{32}^0(2,1) &: 2A_3 + 2A_4 + C_3 + 4C_5 + 2C_6, \\ \mathcal{K}_{32}^0(1,1) &: A_3 + A_4 + 2C_3 + 2C_5 + 4C_6.\end{aligned}\quad (3.2)$$

The 36 kernels are made up of six of each of the types given above. We will show in the next section that, at threshold, all of the diagrams of a particular type are equal. Hence the results of (3.2) at threshold are (including B and D terms)

$$\begin{aligned}\mathcal{K}_{22}^0(1,1) &= 10A + 6B + 4C + 2D, \\ \mathcal{K}_{22}^0(3,1) &= \mathcal{K}_{12}^0(2,1) \\ &= 8A + 6B + 5C + 2D, \\ \mathcal{K}_{12}^0(3,1) &= \mathcal{K}_{32}^0(2,1) \\ &= 4A + 6B + 7C + 2D, \\ \mathcal{K}_{32}^0(1,1) &= 2A + 6B + 8C + 2D.\end{aligned}\quad (3.3)$$

Averaging all of these terms gives us the expected result

$$\bar{\mathcal{K}}^0 = 6A + 6B + 6C + 2D, \quad (3.4)$$

which shows that the average effect of the three body forces in all channels is precisely what would be anticipated from Fig. 11.

B. Size and cancellations in the three body force

The size of the three body terms can easily be estimated at threshold. Using the labeling for momenta given in Fig. 5, we consider the case when

$p=p'=q=q'=0$, $P=3M$, and $M \gg \mu$. Then all of the A diagrams are identical, and equal to

$$\begin{aligned}A &= \frac{ig^6}{8M^3\mu^2} \int \frac{d^4k}{(2\pi)^4} [(\omega_k^2 - k_0^2 - i\epsilon)^2 \\ &\quad \times (k_0 - i\epsilon)^2(-k_0 + i\epsilon)]^{-1},\end{aligned}\quad (3.5)$$

where the $i\epsilon$ prescription in the last factor has been changed to indicate that the spectator pole is not to be included. Straightforward integration gives

$$A = \frac{g^6}{256\pi\mu^5M^3}. \quad (3.6)$$

The same analysis shows that $B = -A$. A more careful estimate would give

$$B + A \simeq A \left[\sqrt{2} \frac{\mu}{M} \right], \quad (3.7)$$

but unfortunately the cancellations are not good enough to eliminate the leading order so this more detailed estimate is unnecessary.

A similar analysis of diagrams C and D gives

$$\begin{aligned}C &= -D \\ &= \frac{ig^6}{(2M)^3} \int \frac{d^4k}{(2\pi)^4} [(\omega_k^2 - k_0^2 - i\epsilon)^3 \\ &\quad \times (k_0 - i\epsilon)^2(-k_0 + i\epsilon)]^{-1} \\ &= A \left(\frac{3}{4} \right).\end{aligned}\quad (3.8)$$

Using these estimates in Eq. (3.4), the average of the three body driving terms obtained above (at threshold) is approximately

$$\bar{\mathcal{K}}^0 = 3A. \quad (3.9)$$

This is a considerable cancellation, but is spoiled by the fact that the number of diagrams of type D is smaller than the number of diagrams of type C . Nevertheless, this result is somewhat smaller than that which would be obtained for the Bethe-Salpeter equation, where only diagrams B and D occur, giving

$$\bar{\mathcal{K}}_{BS}^0 = -\frac{15}{2}A. \quad (3.10)$$

As we shall see in the next section, the cancellation (3.9) is improved slightly once the spurious singularities have been removed from the OPE kernel.

IV. IDENTICAL PARTICLES

In this section we show how the equations simplify and spurious singularities can be removed when the particles are identical. We also present a revised estimate of the three body forces which result after the singularities have been removed, and discuss the significance of the result.

A. The spurious singularities

The singularities which must be removed were referred to briefly in Sec. I. Examine Eq. (2.10) when $j \neq j'$:

$$\begin{aligned} \mu^2 - t(2,3) &= \omega_-^2 - (E_3 + E'_2 - P_{10})^2 \\ &= (\omega_- + E_3 + E'_2 - P_{10}) \\ &\quad \times (\omega_- - E_3 - E'_2 + P_{10}), \end{aligned} \tag{4.1}$$

where

$$\omega_{\pm}^2 = \mu^2 + (\vec{Q}_{\pm} \vec{Q}')^2, \tag{4.2}$$

and we suppress the index i and fix $\vec{Q} = \vec{Q}_i$ in all expressions. The first factor has a singularity when $P_{10} > \omega_- + E_3 + E'_2$, which is due to physical production of mesons and is expected. (See Fig. 13.) The second factor is singular whenever

$$E_3 > \omega_- + P_{10} - E'_2 \tag{4.3}$$

and this is associated with an unphysical instability singularity which arises whenever the off shell nucleon has a mass M^* smaller than $M - \mu$ so that (unphysical) decay of a nucleon into $M^* + \mu$ is possible. Unfortunately, even though this singularity is moved to infinity in the static limit, for actual values of the masses it occurs at too low a momentum to be ignored. In the center of mass (c.m.) system of the interacting pair, the singularity occurs when

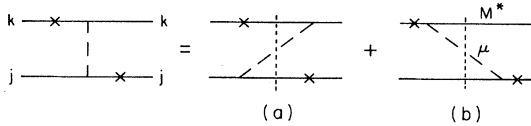


FIG. 13. The singularities of the unsymmetric two body driving term. (a) Normal production singularity. (b) Spurious instability singularity.

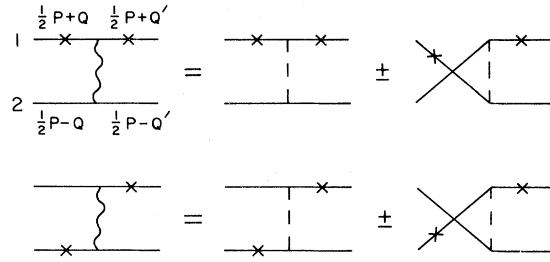


FIG. 14. Exact definition of the symmetrized OPE potentials.

$$\vec{Q}^2 \geq \frac{1}{4}(\mu + W)^2 - M^2, \tag{4.4}$$

which at threshold ($W = 2M$) is about 360 MeV, and is at still smaller \vec{Q}^2 when $W < 2M$, which is possible in the three body system.

This arises from diagrams of type C shown in Fig. 11. One finds that the positive energy spectator pole can overlap the middle meson pole. For external particles on the mass shell, using the momentum labeling given in Fig. 5(b), this occurs when

$$E_k - \frac{1}{3}P_0 - k_0 = \omega_0 - k_0 + \frac{2}{3}P_0 - E'_2 - E_3, \tag{4.5}$$

where

$$\omega_0^2 = \mu^2 + (\vec{q}' + \vec{p}' - \vec{p} - \vec{k})^2. \tag{4.6}$$

This first occurs when $\vec{k} = \vec{q}'$, giving

$$E_3 = \omega_{p',-p} + P_1 - E'_2 \tag{4.7}$$

in agreement with (4.3). We see that the separation of such diagrams into two parts, shown in Figs. 7(b) and (e), has introduced spurious singularities into both parts.

One way to treat this singularity is to redefine the OPE kernel. While the method we will propose might work for nonidentical particles as well, it seems most natural for identical particles.

B. The OPE kernel for identical particles

When working with identical particles, the kernel must always be symmetrized or antisymmetrized.

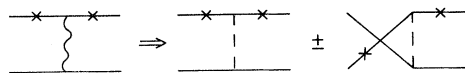


FIG. 15. Prescription for removing the singularity of symmetrized OPE potentials.

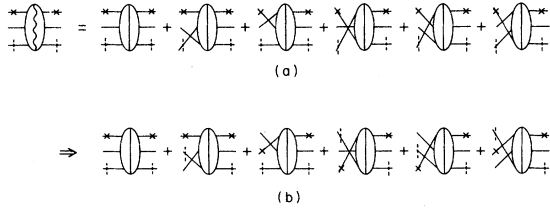


FIG. 16. Symmetrization of the TUF. (a) Exact symmetrization. (b) Generalization of the prescription given in Fig. 15. The \times is the spectator; the line marked with a vertical dash is also on shell but not the spectator.

For the OPE, this symmetrization is shown in Fig. 14, and gives:

$$\begin{aligned}
 V_{22}(\vec{Q}) &= \frac{g^2}{\omega_-^2 - (E_1 - E'_1)^2} \\
 &\quad \pm \frac{g^2}{\omega_+^2 - (E_1 + E'_1 - P_0)^2}, \\
 V_{21}(\vec{Q}) &= \frac{g^2}{\omega_-^2 - (E_2 + E'_1 - P_0)^2} \\
 &\quad \pm \frac{g^2}{\omega_+^2 - (E_2 - E'_1)^2},
 \end{aligned} \tag{4.8}$$

where ω_{\pm} is given in (4.2) and

$$E_{1,2} = [M^2 + (\frac{1}{2}\vec{P}_{\pm}\vec{Q})^2]^{1/2}. \tag{4.9}$$

Note that

$$V_{22}(\vec{Q}) = \pm V_{21}(-\vec{Q}). \tag{4.10}$$

The spurious singularity now occurs in both potentials (4.8), but the symmetry suggests removing the singularity, with the following prescription:

$$\begin{aligned}
 \tilde{V}_{22}(\vec{Q}) &= \tilde{V}_{21}(\vec{Q}) \\
 &= \frac{q^2}{\omega_-^2 - (E_1 - E'_1)^2} \\
 &\quad \pm \frac{g^2}{\omega_+^2 - (E_2 - E'_1)^2}.
 \end{aligned} \tag{4.11}$$

This prescription is shown diagrammatically in Fig. 15. It has made the two potentials identical, and also preserves the symmetry (4.10), which now is also a symmetry of each potential separately.

One of the advantages of the prescription (4.11) is that it is identical to the exact result (4.8) whenever the final state is physical so that $P_0 = E_1 + E_2$. This means that the replacement gives exactly the same result along the elastic cuts, and the small differences arising from the different off shell behavior

can be incorporated into higher order terms. Since we are talking about a two body exchange force, the effect of the prescription (4.11) shows up first in the three body force.

C. Simplification of the equations for identical particles

With the prescription (4.11) the two body driving terms are the same regardless of which of the two particles in the final state are off shell. A glance at Fig. 9 shows that this means that the first six equations collapse immediately down to only three.

The TUF must also be symmetrized for identical particles. The exact symmetrization scheme is shown in Fig. 16(a), where care has been taken to distinguish between the spectator (marked with an \times) and the other mass shell particle (marked with a vertical dashed line). The figure shows that this will involve terms other than the original $\mathcal{X}_{22}^0(1,1)$. In fact, ignoring the arguments of the \mathcal{X}^0 's, we see from Eq. (3.2), where all of the cases which occur in Fig. 16(a) were worked out, that

$$\tilde{\mathcal{X}}_{22}^0(1,1) = 6[6A + 6B + 6C + 2D], \tag{4.12}$$

which displays the fact that on mass shell, when the arguments are all equal, the exact symmetrized TUF will not depend on which of the two particles is on shell.

If we generalize the prescription (4.11) to the TUF in the manner shown in Fig. 16(b), in which the definition depends only on the designation of the initial state, then these TUF, $\tilde{\mathcal{X}}$, will trivially

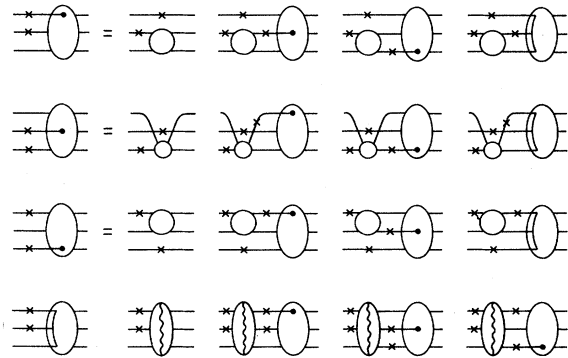


FIG. 17. Diagrammatic representation of the reduced set of four coupled equations to be used with identical particles.

be independent of which particle is off shell and which is the spectator in the final state, even off mass shell. In this case the last six equations reduce immediately to one, in which the three driving terms are now of the symmetrized form

$$\tilde{\mathcal{H}}^0(i') = \frac{1}{2} \sum_{j' \neq i'} \tilde{\mathcal{H}}_{jj'}^0(i, i'). \quad (4.13)$$

We are finally left with the compact set of only four equations drawn in Fig. 17. At first glance, the equations in this figure appear incomplete until one recalls that the \mathcal{S}_j^α no longer depends on j .

D. Additional contributions to \mathcal{H}^0

We now consider how the singularity free prescription for the two body force given in Eq. (4.11) and illustrated in Fig. 15 modifies the three body force. The difference between the exact result and the prescription can be taken into account by including it in a reevaluation of diagrams of type C, which is the only place where the off diagonal potentials which give rise to the problem are to be found.

The corrected contribution C, to be called C', is the difference between the full diagram and a modified diagram in which only the spectator pole is retained and the second meson exchange pole is replaced by a form required by the prescription (4.11) instead of the form given by the diagram [cf. Fig. 5(b)]. Specifically,

$$C' = C - \frac{ig^6}{(2M)^3} \int \frac{d^4k}{(2\pi)^4} \frac{1}{E_k - \frac{1}{3}W - k_0 - i\epsilon} \times \frac{1}{D_1} \left\{ \frac{1}{D_2} - \frac{1}{D_3} \right\}, \quad (4.14)$$

where antinucleon denominators have been replaced by $2M$, and only the spectator pole explicitly shown is to be retained, the other contributions being included in C calculated before. The denominations are

$$\begin{aligned} D_1 &= [E_{k+2p} - 2E + \frac{1}{3}W + k_0] \\ &\quad \times [E_{k+2p'} - 2E + \frac{1}{3}W + k_0] \\ &\quad \times [\omega_{k+p}^2 - k_0^2][\omega_{k+p'}^2 - k_0^2], \\ D_2 &= \omega_{k+2(p+p')}^2 - (\frac{4}{3}W - 4E + k_0)^2, \\ D_3 &= \omega_{k+2(p+p')}^2 - (E_{k+2p} - E_2)^2, \end{aligned} \quad (4.15)$$

where we have relabeled the momenta in Fig. 5(b) by replacing $q' = p'$ with $-p'$, q with $-p$, and p with $2p$. Our configuration corresponds to zero relative momentum for the incoming and outgoing pair. Also, $|\vec{p}| = |\vec{p}'| = \alpha$ and

$$\begin{aligned} E &= (M^2 + \alpha^2)^{1/2}, \\ E_2 &= (M^2 + 4\alpha^2)^{1/2}, \\ W &= 2E + E_2. \end{aligned} \quad (4.16)$$

D_2 is the exact denominator of the pion pole which gives rise to the trouble and D_3 is the application of the prescription to this case. After integrating over k_0 , the two denominators D_2 and D_3 can be combined and the first factor in D_1 canceled, thus completely removing from (4.14) the singularities associated with the elastic cut. This cancellation works because D_2 and D_3 are identical on the elastic cut.

The remainder of the integrand can now be approximated by taking the $M \rightarrow \infty$ limit. If, in addition, we assume α^2 and $\vec{q}^2 = (\vec{p}' - \vec{p})^2$ are small compared to μ^2 , we obtain

$$C' = C \left[1 - \frac{10}{3} \frac{3\alpha^2 - \vec{q}^2}{\mu^2} \right]. \quad (4.17)$$

The correction term vanishes at threshold, but grows rapidly away from threshold. While (4.17) is sufficient for the estimates wanted here, a more detailed treatment is clearly necessary for applications.

If this new result is substituted into the estimate for the average three body force near threshold, (3.4), we obtain

$$\overline{\mathcal{H}}^0 = A \left[3 - 15 \frac{3\alpha^2 - \vec{q}^2}{\mu^2} \right]. \quad (4.18)$$

The correction term has the right sign to reduce the effect of the three body forces considerably, indicating that the prescription for removing the singularities has improved the convergence.

E. Discussion

Our estimates of the size of three body forces derivable from the sum of all ladder and crossed ladder diagrams are very crude, but suggest that the specific size of such effects will be dependent on the details of how the three body problem is handled. All of the contributions discussed in this paper can be considered to be of purely relativistic origin in the sense that no intrinsic three body forces have been considered, and no nucleon isobars or pion resonances have been used to generate the effects. The

forces arise solely from the reduction of pure two body interactions, which might not naively be expected to generate any three body forces at all.

The result (4.18) suggests that the expected cancellation of leading contributions might indeed happen in some average sense. It could also mean that the three body force is a rapidly varying function of momentum transfer and, perhaps, energy.

ACKNOWLEDGMENTS

A large part of the first section of this paper was completed when the author was a summer visitor at

SLAC in 1972, and the support of this laboratory is greatly appreciated. At that time, the author discussed the subject extensively with Etienne Delacroix, who helped develop the presentation of the ideas in Sec. I. The treatment of the spurious singularities was only worked out while the author was a visitor at Carnegie-Mellon, and he greatly appreciates the hospitality of the department during that period. It is a pleasure to acknowledge a helpful conversation with Carl Carlson. The support of the National Science Foundation is gratefully acknowledged.

*Permanent address: Department of Physics, College of William and Mary, Williamsburg, VA 23185.

¹For a review of the literature of three body equations, see *Topics in Current Physics*, edited by A. W. Thomas (Springer, Berlin, 1977), Vol. 2, and references therein.

²F. Gross, Phys. Rev. C 26, 2203 (1982), the preceding

paper; Phys. Rev. 186, 1448 (1969).

³V. A. Alessandrini and R. L. Omnes, Phys. Rev. 139, B167 (1965).

⁴R. Blankenbecler and R. Sugar, Phys. Rev. 142, 1051 (1966).